The American Journal of Pathology, Vol. 170, No. 2, February 2007

DOI: 10.2353/ajpath.2007.060559

Cardiovascular, Pulmonary and Renal Pathology

Development of Immunoglobulin A Nephropathy-Like Disease in β-1,4-Galactosyltransferase-I-Deficient Mice

Toshikazu Nishie,* Osamu Miyaishi,† Haruhito Azuma,‡ Akihiko Kameyama,§ Chie Naruse,* Noriyoshi Hashimoto,* Hitoshi Yokoyama,¶ Hisashi Narimatsu,§ Takashi Wada,¶ and Masahide Asano*

From the Division of Transgenic Animal Science, Advanced Science Research Center, Kanazawa University, Kanazawa; the Department of Pathology,† Aichi Medical University School of Medicine, Aichi; the Department of Urology,‡ Osaka Medical College, Osaka; the Glycogene Function Team,§ Research Center for Glycoscience, National Institute of Advanced Industrial Science and Technology, Ibaraki; and the Department of Disease Control and Homeostasis,¶ Graduate School of Medical Science and Division of Blood Purification, Kanazawa University, Kanazawa, Japan*

β4 Galactosylation of glycoproteins plays important roles in protein conformation, stability, transport, and clearance from the circulation. Recent studies have revealed that aberrant glycosylation causes various human diseases. Here we report that mice lacking β-1,4-galactosyltransferase (β4GalT)-I, which transfers galactose to the terminal *N*-acetylglucosamine of *N*- and *O*-linked glycans in a β-1,4 linkage, spontaneously developed human immunoglobulin A nephropathy (IgAN)-like glomerular lesions with IgA deposition and expanded mesangial matrix. β4GalT-I-deficient mice also showed high serum IgA levels with increased polymeric forms as in human IgAN. IgAN is the most common form of glomerulonephritis, and a significant proportion of patients progress to renal failure. However, pathological molecular mechanisms of IgAN are poorly understood. In humans, abnormal character of serum IgA, especially serum IgA1 with aberrant galactosylation and sialylation of *O*-glycans in its hinge region is thought to contribute to the pathogenesis of IgAN. Mouse IgA has *N*-glycans but not *O*-glycans, and β4-galactosylation and sialylation of the *N*-glycans on the serum IgA from β4GalT-I-deficient mice was completely absent. This is the first report demonstrating that genetic remodeling of protein glycosylation causes IgAN. We propose that carbohydrates of serum IgA are involved in the development of IgAN, whether the carbohydrates are *O*-glycans or *N*-glycans. ***(Am J Pathol 2007, 170:447–456; DOI: 10.2353/ajpath.2007.060559)***

The glycosylation of glycoproteins is important for their biological activities, conformation, stability, transport, and clearance from the circulation, and cell-surface glycans participate in cell-cell and cell-matrix interactions. Recent studies also indicate that aberrant glycosylation causes various human disorders, such as metastasis of tumor cells, muscular dystrophy, and dyserythropoietic anemia.[1–3] Carbohydrates are also involved in infectious diseases including influenza virus,[4] *Helicobacter pylori*,[5] and trypanosomes.[6] The congenital disorders of glycosylation (CDG) are inherited multisystemic disorders characterized by the defective glycosylation of glycoproteins attributable to mutations in genes required for the biosynthesis of *N*-glycans.[7]

β-1,4-Galactosyltransferases (β4GalTs) transfer galactose (Gal) from UDP-Gal to terminal *N*-acethylglucosamine (GlcNAc) of *N*- and *O*-glycans in a β-1,4 linkage to synthesize the Galβ1-4GlcNAc structure.[8] The β4GalT-I gene was initially identified from bovine, human, and murine[9–11] among glycosyltransferases. So far, seven β4GalT genes (β4GalT-I to β4GalT-VII) have been isolated,[8] and their individual roles are being investigated. β4GalT-I is expressed ubiquitously and strongly in almost all tissues except neural tissues, suggesting that β4GalT-I is involved in β4 galactosylation of many glycoproteins. β4 galactosylation of glycoproteins is widely distributed in mammalian tissues and is involved in vari-

Supported by the Mizutani Foundation for Glycoscience (grant no. 040051); the Ministry of Education, Science, Sports, and Culture of Japan (grant no. 17046005); and the Japan Society for the Promotion of Science (grant no. 175556).

Accepted for publication October 17, 2006.

Address reprint requests to Masahide Asano, Division of Transgenic Animal Science, Advanced Science Research Center, Kanazawa University, 13-1 Takara-machi, Kanazawa 920-8640, Japan. E-mail: asano@kiea.m.kanazawa-u.ac.jp.

ous physiological functions through interactions with selectins, galectins, asialoglycoprotein receptor, and so on. Previously, to elucidate the role of β4 galactosylation *in vivo*, we and another group generated mice lacking β4GalT-I.[12,13] Serum glycoproteins are primarily deficient in β4 galactosylation, whereas neural glycoproteins are not affected in β4GalT-I$^{-/-}$ mice.[12,13] The β4GalT-I$^{-/-}$ mice show semilethality before weaning because of growth retardation[12] as well as reduced inflammatory responses[14] and delayed skin wound healing[15] attributable to impaired leukocyte infiltration caused by the reduced biosynthesis of selectin ligands. In addition, it is suggested that β4 galactosylation is important in anterior pituitary hormone function.[13]

Immunoglobulin A nephropathy (IgAN) is the most common glomerulonephritis worldwide, and a significant proportion (20 to 30%) of patients progress to renal failure 10 to 20 years after the onset of the disease.[16,17] Histologically, IgAN is characterized by glomerular mesangial expansion and IgA1 deposition, often with C3 and sometimes with IgG and IgM deposition.[18] Clinically, hematuria and proteinuria are typically observed, and high serum IgA levels are often detected in patients with the disease.[19] Pathological roles for the abnormal serum IgA, including an increase in circulating polymeric IgA, the formation of immune complexes containing IgA, and the abnormal galactosylation and sialylation of *O*-glycans of IgA, have been proposed. However, the pathological molecular mechanisms remain to be fully elucidated.

Here, we investigated the disorder of the β4GalT-I$^{-/-}$ mice in more detail. After weaning, the surviving β4GalT-I$^{-/-}$ mice developed similarly to β4GalT-I$^{+/-}$ mice, but they began to die sporadically from 10 weeks of age. Necropsy revealed that the kidney was small and pale. Histological examination of the kidney showed that β4GalT-I$^{-/-}$ mice developed IgAN-like disease consistent with the pathological diagnosis of human IgAN, including IgA deposition, expanded mesangial matrix, and electron-dense deposits in the paramesangial regions. Furthermore, the β4GalT-I$^{-/-}$ mice showed high serum IgA levels with increased polymeric forms. As expected, β4 galactosylation on the *N*-glycans of the serum IgA of the β4GalT-I$^{-/-}$ mice was completely absent. This is the first report demonstrating that genetic remodeling of protein glycosylation causes IgAN. Aberrant *O*-glycosylation on human IgA1 has been suggested to be involved in the pathogenesis of human IgAN.[20–24] Although *N*-glycans, but not *O*-glycans, are attached to mouse IgA, pathological roles of aberrant galactosylation on IgA in the development of IgAN in humans and mice are discussed.

Materials and Methods

Mice

β4GalT-I$^{-/-}$ mice on a mixed 129/Sv and C57BL/6 background were used for the experiments, with sex-matched β4GalT-I$^{+/-}$ littermates as controls.[12,14,15] The mice were kept in an environmentally controlled clean room at the Institute for Experimental Animals, Advanced Science Research Center, Kanazawa University. Experiments were conducted according to guidelines for the care and use of laboratory animals in Kanazawa University and safety guidelines for gene manipulation experiments.

Histological Analysis

Kidneys were fixed in 10% neutral buffered formalin, dehydrated, and embedded in paraffin according to standard procedures. Paraffin sections (4 to 6 μm thick) were deparaffinized, rehydrated, and subjected to hematoxylin and eosin (H&E), periodic acid-Schiff (PAS), periodic acid-methenamine-silver (PAM), and Masson's trichrome staining using standard methods. The degree of glomerular lesions was classified into minor glomerular abnormality, segmental lesion, and global lesion by investigating PAS-stained sections. The segmental lesion includes segmental glomerular sclerosis, focal adhesion, and small crescent formation, whereas the global lesion includes global mesangial matrix expansion. Approximately 100 glomeruli per mouse from one to two β4GalT-I$^{+/-}$ mice and two to three β4GalT-I$^{-/-}$ mice at each stage of age were evaluated. The extent of glomerular sclerosis was expressed as a percentage of the PAM-positive area per whole glomerular area as described previously.[25] At each stage of age, ~10 glomeruli per mouse from one to two β4GalT-I$^{+/-}$ mice and two to three β4GalT-I$^{-/-}$ mice were used for the measurement. Each area was measured by computer-aided manipulation using Mac Scope version 6.02 (Mitani Shoji Co., Ltd., Fukui, Japan).

For immunofluorescence microscopy, frozen kidney sections (5 μm thick) were prepared. The slides were washed and treated with SuperBlock blocking buffer (Pierce Biotechnology, Inc., Rockford, IL). They were incubated with goat anti-mouse IgA (Southern Biotechnology Associates, Birmingham, AL), IgG, IgM, or C3 Fab fragment (ICN/Cappel, Aurora, OH). They were then incubated with fluorescein isothiocyanate-conjugated rabbit anti-goat IgG antibody (Sigma Aldrich, St. Louis, MO). The degree of IgA and C3 deposition in glomeruli was evaluated by arbitrary score (−, +/−, +, ++, +++) using 50 to 100 glomeruli per mouse from two β4GalT-I$^{+/-}$ mice and two β4GalT-I$^{-/-}$ mice at each stage of age.

Electron Microscopy

Kidneys from β4GalT-I$^{-/-}$ mice were fixed with glutaraldehyde and osmium tetroxide, embedded in Epon 812 (Oken Shoji Co., Tokyo, Japan), sliced into 0.1-μm sections, double-stained with uranyl acetate and lead citrate, and examined under the electron microscope (Hitachi H-600; Hitachi Co., Tokyo, Japan).[26]

Urinalysis

Urine samples were collected and tested for hematuria using Uropaper II (Eiken Chemical Co., Ltd., Tokyo, Ja-

pan). Urinary albumin levels were determined by a double-sandwich enzyme-linked immunosorbent assay (ELISA) using affinity-purified goat anti-mouse albumin antibody and horseradish peroxidase (HRP)-conjugated goat anti-mouse albumin antibody (Bethyl Laboratories, Montgomery, TX). HRP activity was detected by 2,2′-azino-bis(3-ethylbenz-thiazoline-6-sulfonic acid) (ABTS) substrate and measured using microplate reader model 550 (Bio-Rad, Hercules, CA).

Measurement of Immunoglobulin Levels

IgG, IgM, and IgA levels were measured according to the published protocol for sandwich ELISA[27] with some modifications. Briefly, affinity-purified goat anti-mouse Ig (G + M + A) antibody (ICN/Cappel) for IgG and IgM titrations or affinity-purified goat anti-mouse IgA antibody for IgA titration was added to 96-well plates. The plates were blocked with Block Ace (Yukijirushi, Sapporo, Japan) to prevent nonspecific binding, and then serially diluted serum samples or fecal extracts were added. Fecal samples were collected and dissolved at a concentration of 100 mg/ml in phosphate-buffered saline containing complete protease inhibitors and NaN_3. Then, fecal extracts were prepared after vigorous vortex and centrifugation of the samples. After the plates were incubated, immunoglobulins were detected with HRP-conjugated goat anti-mouse IgG, IgM, or IgA antibody (ICN/Cappel) and ABTS.

Detection of Autoantibody Against Double-Stranded (ds) DNA

Ninety-six-well plates were coated with 50 mg/ml poly-L-lysine and washed. The plates were applied with 5.0 mg/ml of dsDNA in Tris-buffered saline and then masked with 50 mg/ml of poly-L-glutamic acid. Serial dilutions of serum were added to the plates, followed by a HRP-conjugated goat anti-mouse IgG or IgA.

Gel Filtration Assay

Gel filtration of the serum proteins was performed with the SMART system (Amersham Pharmacia Biotech, Piscataway, NJ) using a Superdex 200 PC 3.2/30 column and buffer/eluent (0.05 mol/L phosphate buffer containing 0.15 mol/L NaCl, pH 7.0) with a flow rate of 40 μl/minute. Fractions of 30 μl were collected after 0.5 ml of eluent. The IgA concentration of each fraction was determined by ELISA.

Western Blot Analysis

Proteins in the IgA-containing fractions obtained by the gel filtration, above, were separated by sodium dodecyl sulfate-polyacrylamide gel electrophoresis according to the method of Laemmli.[28] Samples from each fraction were mixed with an equal volume of 0.125 mol/L Tris-HCl (pH 6.8), 4% sodium dodecyl sulfate, 10% sucrose, and 0.004% bromphenol blue. These mixtures were boiled for 3 minutes in the presence of 2-mercaptoethanol for reducing conditions or incubated for 30 minutes at room temperature in the absence of 2-mercaptoethanol for nonreducing conditions. After electrophoresis, the proteins on the gel were transferred to a polyvinylidene difluoride membrane (Millipore Corp., Bedford, MA) by electroblotting. The membrane was incubated with Block Ace and then with goat anti-mouse IgA antibody. After incubation, the membrane was treated with biotin-conjugated rabbit anti-goat IgG antibody (Vector Laboratories, Burlingame, CA) and then with avidin-HRP (Amersham Pharmacia Biotech). Finally, the membrane was soaked in ECL reagent (Amersham Pharmacia Biotech) and exposed to X-ray film or lumino imaging analyzer FAS-1100 (Toyobo Corp., Osaka, Japan).

Matrix-Assisted Laser-Desorption Ionization Time-of-Flight Mass Spectrometry (MALDI-TOF MS) Analysis

N-glycans from IgA were prepared as described.[29] Sialidase digestion of *N*-glycans was performed with *Arthrobacter ureafanciencs* sialidase (Marukin Bio Co., Ltd., Kyoto, Japan). Mass measurements were performed using a Reflex IV TOF-MS equipped with a pulsed ion extraction system (Bruker-Altonik GmbH, Bremen, Germany). Ions were generated by a pulsed 337-nm nitrogen laser and were accelerated to 20 kV. All of the spectra were obtained using a reflectron mode with delayed extraction of 200 ns and were the result of signal averaging of 200 laser shots. For sample preparation, 0.5 ml of an analyte solution was deposited on the target plate and allowed to dry. Then, 0.5 ml of 2,5-DHB (Bruker-Daltonik, Bremen, Germany) solution (10 mg/ml in 20% ethanol) was used to cover the matrix on the target plate and allowed to dry.

Statistics

The results are expressed as means ± SD. Statistical evaluation was performed by means of Student's *t*-test or Welch's *t*-test after Levene's test for equality of variance between β4GalT-I-deficient and control mice. A two-sided level of $P < 0.05$ was accepted as statistically significant.

Results

Impaired Renal Function in β4GalT-I$^{-/-}$ Mice

Urinary parameters such as albuminuria and hematuria were examined in the β4GalT-I$^{-/-}$ mice. The urinary albumin concentration was markedly higher in the β4GalT-I$^{-/-}$ mice than in β4GalT-I$^{+/-}$ mice (Figure 1A). Hematuria was also detected in some of the β4GalT-I$^{-/-}$ mice, and the ratio of hematuria increased with age, whereas no hematuria was observed in the β4GalT-I$^{+/-}$ mice at any age examined (Figure 1B).

A

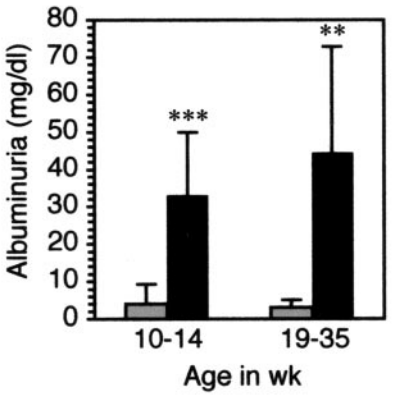

B

Hematuria (positive / total)

Genotype	Age in wk		
	11-14	15-22	24-41
+/-	0/18	0/19	0/24
-/-	2/18	4/19	5/24

Figure 1. Urinary parameters in β4GalT-I$^{-/-}$ mice. Increase of urinary albumin levels and hematuria with age in β4GalT-I$^{-/-}$ mice. **A:** Urinary albumin levels in β4GalT-I$^{+/-}$ (**gray bars**) and β4GalT-I$^{-/-}$ mice (**black bars**) at 10 to 14 (+/−, $n = 19$; −/−, $n = 16$) and 19 to 35 (+/−, $n = 9$; −/−, $n = 9$) weeks of age. The results are expressed as means ± SD. $^{**}P < 0.01$, $^{***}P < 0.001$. **B:** Hematuria was tested using uropaper in β4GalT-I$^{+/-}$ and β4GalT-I$^{-/-}$ mice at each week of age.

Mesangial Matrix Expansion and Mesangial Deposition in β4GalT-I$^{-/-}$ Mice

We examined the kidneys of β4GalT-I$^{-/-}$ mice histologically. Many glomeruli were affected with marked expansion of the mesangial matrix in β4GalT-I$^{-/-}$ mice (Figure 2B). Representative injured glomeruli are shown (Figure 2, F–H). Acellular eosinophilic lesions are seen near the vascular pole of the glomerulus, indicating expansion of the mesangial matrix (Figure 2F). The capillary lumens were collapsed, and there was marked expansion of the mesangial matrix. The expanded mesangial matrix was positively stained by PAS reagent (Figure 2G). With Masson's trichrome, brilliant reddish staining was detected in the mesangial area (Figure 2H), suggesting the deposition of immune complexes in the mesangial area. No remarkable differences from wild-type mice were detected in the β4GalT-I$^{+/-}$ mice by any of the histochemical methods used (Figure 2, A, C–E). The degree of glomerular lesion was classified into minor glomerular abnormality, segmental lesion and global lesion, and evaluated at each age (Figure 2I). Approximately 75% of glomeruli in β4GalT-I$^{-/-}$ mice were already affected at younger age (8 to 13 weeks), and the ratio of glomeruli with global lesion increased with age. The ratio of segmental lesion in β4GalT-I$^{+/-}$ mice slightly increased with age, but ~75% of glomeruli displayed minor glomerular abnormality at older age (47 to 48 weeks), when almost all glomeruli were affected in β4GalT-I$^{-/-}$ mice.

We further quantified the extent of glomerular sclerosis in β4GalT-I$^{-/-}$ mice to examine the disease progression with age. The extent of glomerular sclerosis expressed as a percentage of the PAM-positive area per whole glomerular area in β4GalT-I$^{-/-}$ mice was approximately twofold higher at younger age (8 to 20 weeks; Figure 3, C and E) and approximately threefold higher at older age (24 to 48 weeks; Figure 3, D and E) than those in β4GalT-I$^{+/-}$ mice (Figure 3, A, B, and E), whereas that in β4GalT-I$^{+/-}$ mice did not change with age. Glomerulomegaly was also observed in β4GalT-I$^{-/-}$ mice, suggesting the possible presence of hyperfiltration of the glomeruli (Figure 3, C and D).

Predominant Mesangial IgA, as Well as IgG, IgM, and C3 Deposits in β4GalT-I$^{-/-}$ Mice

To examine the content of the mesangial deposits in the glomeruli of β4GalT-I$^{-/-}$ mice, we performed immunofluorescence microscopy using anti-IgA, anti-C3, anti-IgM, and anti-IgG antibodies. IgA deposition was detected in most glomeruli of β4GalT-I$^{-/-}$ mice, whereas only faint signals were detected in β4GalT-I$^{+/-}$ mice (Figure 4, A–C, G). IgA was brilliantly stained in the mesangial area of the glomeruli, whereas IgG was occasionally detected in the area (Figure 4, G and J). The C3 deposition was more diffuse than the IgG staining, but the signal was weaker than that of IgA or IgM (Figure 4, G–J). All of the immune components were only barely detectable in the β4GalT$^{+/-}$ mice (Figure 4, C–F). The degree of glomerular IgA and C3 deposition with age is shown in Table 1. Strong signals (++ and +++) of IgA and C3 were detected in approximately half of glomeruli in β4GalT-I$^{-/-}$ mice, whereas no signal (−) or weak signals (+/− and +) were detected in almost all glomeruli in β4GalT-I$^{+/-}$ mice. To examine the precise localization of the immune complexes, we observed the glomeruli of the β4GalT-I$^{-/-}$ mice by electron microscopy. Electron-dense deposits were specifically detected in the paramesangial areas (Figure 4K). No remarkable changes were detected in other parts of the glomeruli, such as the capillary basement membrane and endothelial cells. Taken together, these histological and immunohistochemical results show that the β4GalT-I$^{-/-}$ mice developed human IgAN-like glomerular lesions.

High Serum IgA Levels in β4GalT-I$^{-/-}$ Mice

Because high serum IgA levels are often observed in human IgAN,[30] the concentrations of serum immunoglobulin classes in the β4GalT-I$^{+/-}$ and β4GalT-I$^{-/-}$ mice were measured. Serum IgA levels in the β4GalT-I$^{-/-}$ mice increased with age and were markedly higher than those in β4GalT-I$^{+/-}$ mice at any age examined (Figure 5A). In contrast, there was no significant difference between the serum IgG levels of the two groups at any age (Figure 5B). Serum IgM levels of the β4GalT-I$^{-/-}$ mice at 12 to 13 weeks were approximately twofold higher than

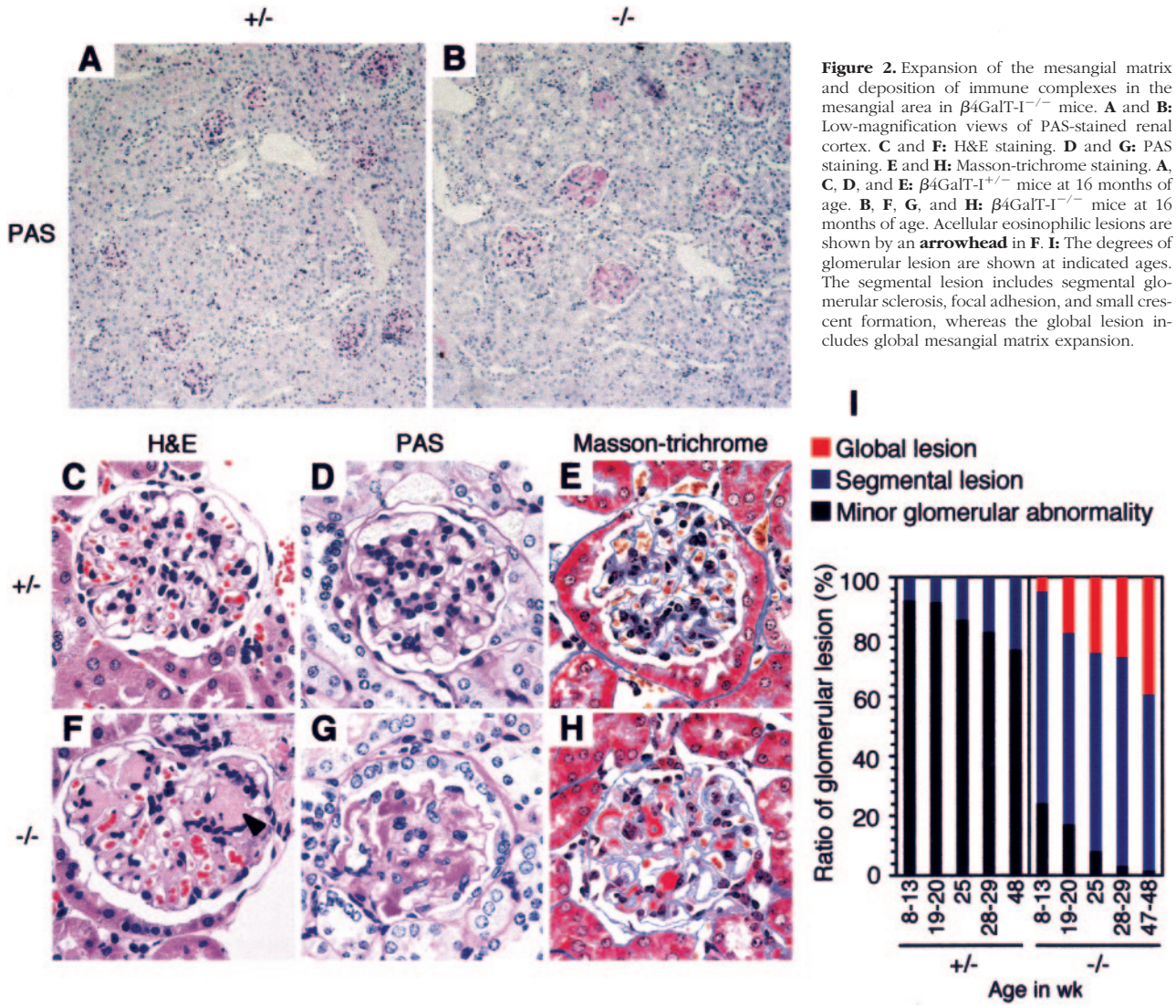

Figure 2. Expansion of the mesangial matrix and deposition of immune complexes in the mesangial area in β4GalT-I$^{-/-}$ mice. **A** and **B:** Low-magnification views of PAS-stained renal cortex. **C** and **F:** H&E staining. **D** and **G:** PAS staining. **E** and **H:** Masson-trichrome staining. **A**, **C**, **D**, and **E:** β4GalT-I$^{+/-}$ mice at 16 months of age. **B**, **F**, **G**, and **H:** β4GalT-I$^{-/-}$ mice at 16 months of age. Acellular eosinophilic lesions are shown by an **arrowhead** in **F**. **I:** The degrees of glomerular lesion are shown at indicated ages. The segmental lesion includes segmental glomerular sclerosis, focal adhesion, and small crescent formation, whereas the global lesion includes global mesangial matrix expansion.

those of the β4GalT-I$^{+/-}$ mice, whereas those of the β4GalT-I$^{-/-}$ mice at 24 to 28 weeks were approximately half those of the β4GalT-I$^{+/-}$ mice (Figure 5C). Furthermore, we measured serum IgG- and IgA-type autoantibodies against dsDNA (Figure 5D). Serum IgG levels against dsDNA were very low in both the β4GalT-I$^{+/-}$ and β4GalT-I$^{-/-}$ mice (Figure 5D, left). Serum IgA levels against dsDNA in the β4GalT-I$^{-/-}$ mice were slightly higher than those in the β4GalT-I$^{+/-}$ mice but were still very low, and the difference was not significant (Figure 5D, right).

Increased Ratio of Polymeric Serum IgA in β4GalT-I$^{-/-}$ Mice

To examine the forms of the serum IgA, we fractionated the serum proteins by gel filtration and measured the IgA levels in each fraction. Serum from β4GalT-I$^{+/-}$ mice gave one major (fraction 25) and one minor (fraction 20) IgA peak (Figure 6A). In contrast, serum from β4GalT-I$^{-/-}$ mice had two IgA peaks, at fractions 20 and 25 and an additional minor peak around fraction 16 (Figure 6B). To confirm the IgA levels of each fraction, we performed Western blotting for fractions 16, 20, and 25 from each genotype under reducing conditions using an antibody against the mouse IgA heavy chain. IgA from the β4GalT-I$^{+/-}$ mice was detected rarely or only at low levels in fractions 16 and 20, respectively, whereas the IgA from β4GalT-I$^{-/-}$ mice was readily detectable in these fractions (Figure 6C). The Western blot analysis was also performed under nonreducing conditions for fractions 16, 20, and 25. The IgA molecules in fraction 25 from each genotype consisted of two bands, which were the monomeric (H_2L_2) and half molecule (HL) forms, as judged by their molecular weights (Figure 6D). The IgA molecules from the β4GalT-I$^{-/-}$ mice in fractions 20 and 16 were, respectively, dimeric and higher order polymeric forms. The polymer band in fraction 16 from β4GalT-I$^{-/-}$ mice was faint (Figure 6D) compared with the IgA band of the same sample in Figure 6C, probably because of the inefficient transmission of high-molecular weight proteins to the membrane. These dimeric and polymeric forms of

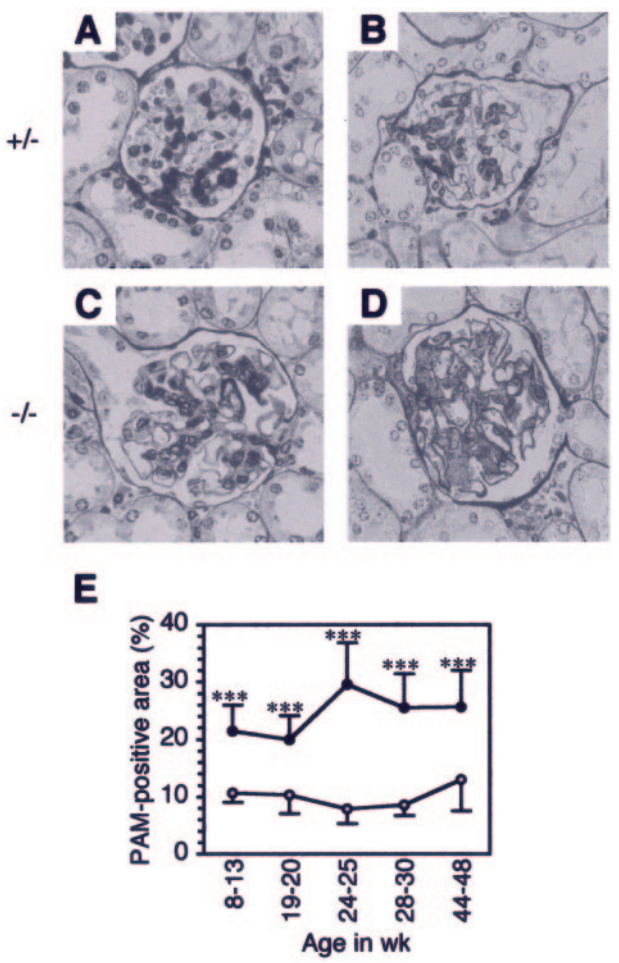

Figure 3. Age-dependent progression of glomerular sclerosis in β4GalT-I$^{-/-}$ mice. **A–D:** PAM staining. β4GalT-I$^{+/-}$ mice at 19 weeks of age (**A**) and 29 weeks of age (**B**), and β4GalT-I$^{-/-}$ mice at 19 weeks of age (**C**) and 29 weeks of age (**D**). **E:** PAM-positive area in β4GalT-I$^{+/-}$ (**gray circles**) and β4GalT-I$^{-/-}$ mice (**black circles**) at 8 to 13, 19 to 20, 24 to 25, 28 to 30, and 44 to 48 weeks of age. The results are expressed as means ± SD. ***$P <$ 0.001.

IgA were, respectively, slightly and rarely detectable in β4GalT-I$^{+/-}$ mice (Figure 6D). These results indicate that dimeric and polymeric serum IgAs were unusually abundant in the β4GalT-I$^{-/-}$ mice.

Serum polymeric IgA in β4GalT-I$^{-/-}$ mice might originate from gut-associated lymphoid tissues, which produced intestinal dimeric and polymeric IgA. We measured IgA levels in fecal extracts from β4GalT-I$^{+/-}$ and β4GalT-I$^{-/-}$ mice (Figure 5E) to examine whether transepithelial transport of polymeric IgA into the gut lumen was impaired. No significant difference was observed in fecal IgA levels from each genotype.

Lack of the Sialyl Gal Structure on IgA from β4GalT-I$^{-/-}$ Mice

To examine whether *N*-glycans attached to IgA in the β4GalT-I$^{-/-}$ mice are Gal-deficient, we analyzed them with MALDI-TOF MS. Based on the previous report[31] that *N*-glycans of IgA in wild-type mice are the sialylated bi- and tri-antennary complex-type glycans, we interpreted the observed signals in the mass spectra (Figure 7C). Acidic glycans, such as the sialylated *N*-glycans, generally give poor MALDI mass spectra.[32] Therefore, we acquired the mass spectra of *N*-glycans before and after sialidase digestion. The *N*-glycans released from IgA in the β4GalT-I$^{-/-}$ mice were completely absent of Gal (Figure 7B), whereas those from IgA in β4GalT-I$^{+/-}$ mice were partially galactosylated and all galactosylated glycans were further extended with sialic acid (Figure 7A). These results indicated the *N*-glycans on IgA from the β4GalT-I$^{-/-}$ were completely lacking in sialyl Gal residues.

Discussion

We demonstrate here that the β4GalT-I$^{-/-}$ mice developed an IgAN-like disease consistent with the pathological diagnosis of human IgAN, including mesangial IgA deposition, mesangial matrix expansion and electron-dense deposits in the paramesangial regions. Glomerular sclerosis was observed at 8 weeks of age and progressed with age. Furthermore, the β4GalT-I$^{-/-}$ mice showed high serum IgA levels and an increased proportion of polymeric IgA, which are also similar to the features of human IgAN. However, hematuria was observed in only some of the β4GalT-I$^{-/-}$ mice, which is not consistent with human IgAN. The difference might be explained by reduced inflammatory responses attributable to the impaired biosynthesis of selectin ligands in the β4GalT-I$^{-/-}$ mice[14,15] because hematuria is induced by inflammation.[33] In fact, there was no detectable infiltration of inflammatory cells into the renal glomerular and interstitial regions of the β4GalT-I$^{-/-}$ mice (unpublished data). Therefore, the β4GalT-I$^{-/-}$ mouse is a novel disease model that has most of the pathological and clinical features of human IgAN except hematuria.

So far, several transgenic animal models for human IgAN have been developed, including a mouse lacking uteroglobin (UG), an anti-inflammatory protein,[34] and a transgenic mouse expressing the human Fcα receptor (FcαR) on macrophages/monocytes.[35] Moreover, it was recently reported that mice transgenic for Light, a ligand for lymphotoxin β receptor, develop severe intestinal inflammation, leading to high serum polymeric IgA levels attributable to overproduction of polymeric IgA in the intestine and impaired intestinal transportation, and develop IgAN.[36] Unlike Light transgenic mice, however, obvious intestinal inflammation was not observed, and fecal IgA levels were normal in the β4GalT-I$^{-/-}$ mice (unpublished data and Figure 5E).

In terms of the genetic remodeling of protein glycosylation, α-mannosidase II-deficient mice are reported to develop an autoimmune disease similar to human lupus nephritis.[37] Because lupus nephritis is similar to IgAN in some aspects and α-mannosidase II is involved in the biosynthesis of *N*-glycans upstream of β4GalT-I, we measured autoantibodies against dsDNA. The serum IgG and IgA titers against dsDNA in β4GalT-I$^{-/-}$ mice were com-

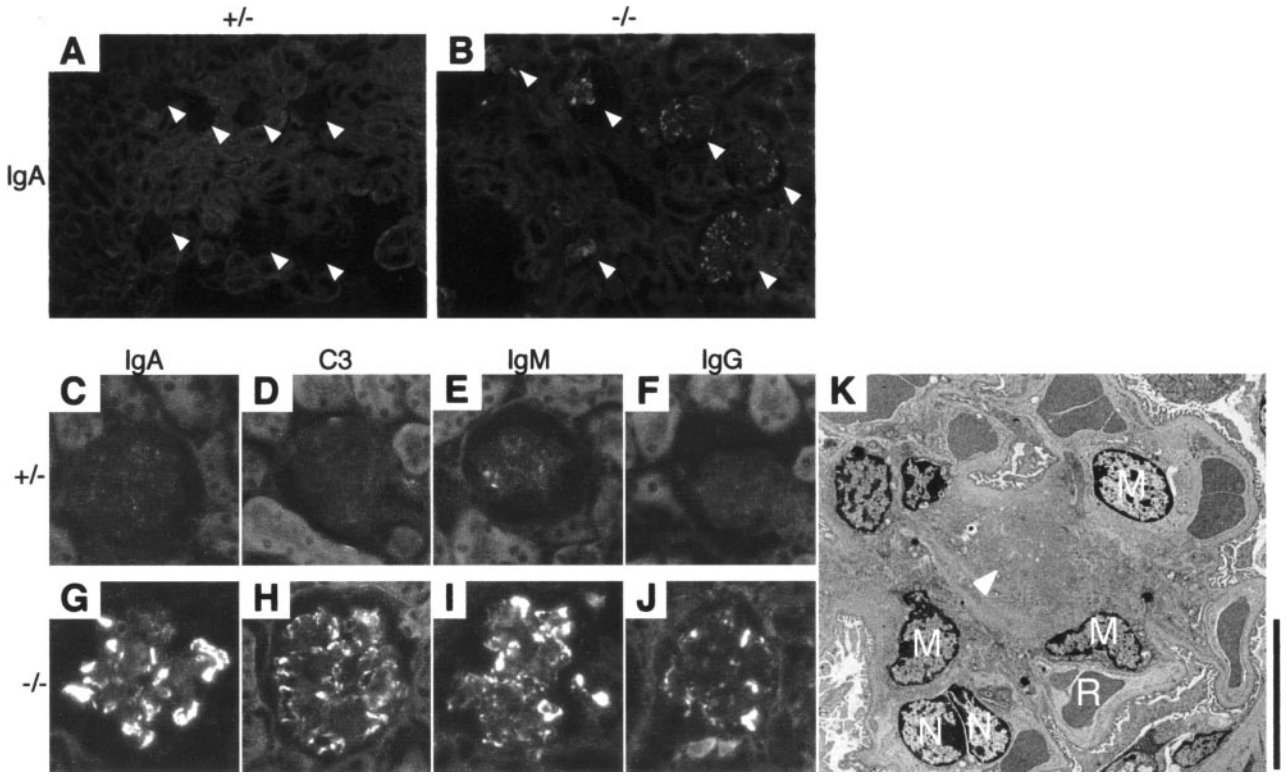

Figure 4. Predominant mesangial IgA, C3, IgM, and IgG deposits in β4GalT-I$^{-/-}$ mice. Immunofluorescence microscopic analysis of frozen kidney sections using antibodies against IgA, C3, IgM, and IgG was performed. **A** and **B:** β4GalT-I$^{+/-}$ mice and β4GalT-I$^{-/-}$ littermates at 20 weeks of age, respectively. **Arrowheads** indicate glomeruli. **C–F:** β4GalT-I$^{+/-}$ mice at 25 weeks of age; **G–J:** β4GalT-I$^{-/-}$ littermates. **A**, **B**, **C**, **G:** IgA; **D**, **H:** C3; **E**, **I:** IgM; and **F**, **J:** IgG. **K:** Deposition of electron-dense materials in the paramesangial areas of the glomeruli. Kidney from β4GalT-I$^{-/-}$ mice at 37 weeks of age was collected, and electron microscopic analysis was performed. **Arrowhead**, an electron-dense deposit; M, mesangial cells; N, endothelial cells; R, red blood cells. Scale bar = 10 μm.

parable with those of β4GalT-I$^{+/-}$ mice (Figure 5D). Thus, the β4GalT-I$^{-/-}$ mice did not develop lupus nephritis.

Dimeric and polymeric serum IgA were unusually abundant in the β4GalT-I$^{-/-}$ mice. It is unlikely that the polymeric IgA was derived from gut-associated lymphoid tissues that mainly produce polymeric IgA because transepithelial transport of IgA into the gut lumen was normal in the β4GalT-I$^{-/-}$ mice. Mutant human IgA1 molecule lacking the *N*-glycosylation sites tends to form higher polymeric forms.[38] Of interest, the Gal residues of *N*-glycans are deficient on more than 50% of the secretory polymeric IgA in human colostrum.[39] Polymeric IgA easily forms immune complexes because of its multivalent properties, and then these macromolecular complexes are trapped in the glomeruli when injected into mice.[40] Therefore, it is most likely that asialo-agalacto IgA tends to form aggregates, and the increased polymeric IgA in the β4GalT-I$^{-/-}$ mice may accumulate in the glomeruli.

Hyper serum IgA might also contribute to the development of IgAN in the β4GalT-I$^{-/-}$ mice. We examined the number of IgA-producing cells in lymphoid tissues including spleens, mesenteric lymph nodes, Peyer's patches, lamina propria, and bone marrows as well as blood clearance of each serum IgA in wild-type mice, but no significant difference between β4GalT-I$^{+/-}$ and β4GalT-I$^{-/-}$ mice was detected (unpublished data). The cause of hyper serum IgA in the β4GalT-I$^{-/-}$ mice still remains to be elucidated.

A hyper IgA (HIGA) mouse, a mouse model for human IgAN with high serum IgA levels,[41] also shows reduced

Table 1. Degree of IgA and C3 Deposition with Age

Genotype	Degree of IgA and C3 deposition (%)										
		IgA					C3				
	Age (weeks)	−	+/−*	+	++	+++	−	+/−*	+	++	+++
+/−	11	57	29	13	1	0	17	66	14	3	0
	19 to 20	49	22	28	1	0	37	48	15	0	0
	27 to 30	43	11	34	11	1	25	63	12	0	0
−/−	11	16	12	31	41	0	10	24	28	38	0
	19 to 20	20	7	27	37	9	14	15	32	38	1
	27 to 30	11	8	31	36	14	9	32	34	23	2

*+/− indicates quite weak, but not negligible signal.

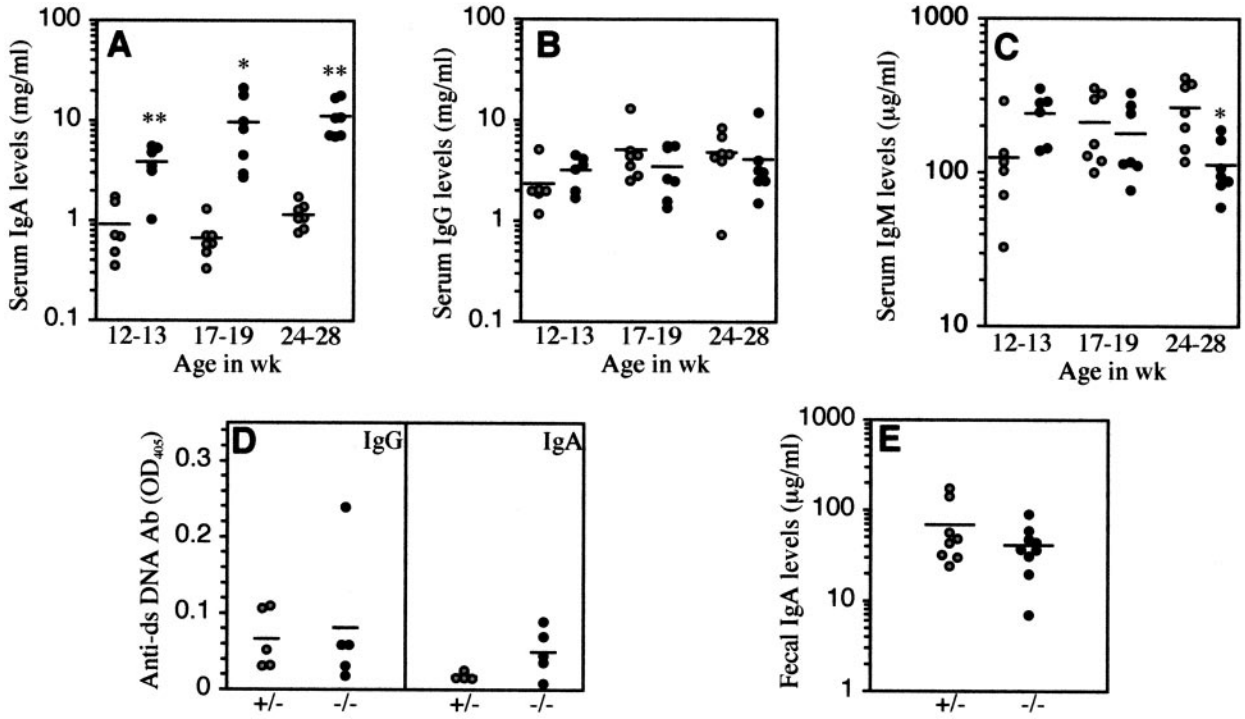

Figure 5. Significant increase of serum IgA levels in β4GalT-I$^{-/-}$ mice. Serum IgA (**A**), IgG (**B**), and IgM (**C**) levels from β4GalT-I$^{+/-}$ ($n = 6$ or 7, **gray circles**) and β4GalT-I$^{-/-}$ ($n = 6$ or 7, **black circles**) mice at each week of age. **D:** Serum IgG (left) and IgA (right) levels against dsDNA from β4GalT-I$^{+/-}$ ($n = 5$, **gray circles**) and β4GalT-I$^{-/-}$ ($n = 5$, **black circles**) mice at 5 to 7 months of age. **E:** Fecal IgA levels in β4GalT-I$^{+/-}$ ($n = 7$, **gray circles**) and β4GalT-I$^{-/-}$ ($n = 8$, **black circles**) mice at 10 to 15 weeks of age. $^{*}P < 0.05$, $^{**}P < 0.01$.

galactosylation of the *N*-glycans on serum IgA.[42] It has been recently reported that F1-bcl-2 transgenic mice [New Zealand White (NZW) × C57BL/6], which develop both IgAN-like and autoimmune lupus-like diseases, show reduced levels of galactosylation and sialylation of serum IgA.[43] These results support our hypothesis that aberrant *N*-glycosylation of IgA is involved in the pathogenesis of IgAN. However, we cannot exclude the possibility that IgAN in β4GalT-I$^{-/-}$ mice was caused by other mechanisms, because many glycoproteins were impaired in β4 galactosylation. For example, aberrant glycosylation of mesangial IgA receptors such as FcαRI (CD89), Fcα/μ receptor and transferrin receptor[44] might cause abnormal IgA deposition in the glomeruli. Human IgA1, a major subtype of serum IgA, has two *N*-glycosylation sites in its CH2 and C-terminal regions and several *O*-glycosylation sites in its hinge region.[45] Aberrant *O*-

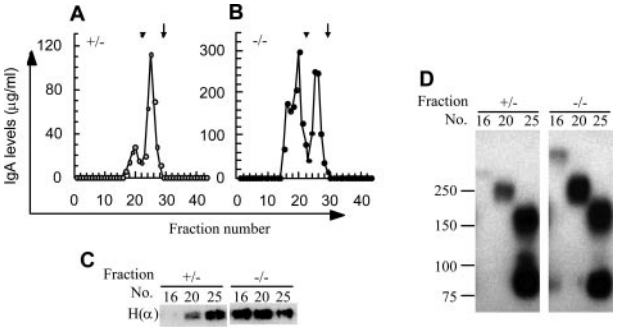

Figure 6. Increased proportion of dimeric and polymeric IgA in sera of β4GalT-I$^{-/-}$ mice was observed. **A** and **B:** Serum proteins from β4GalT-I$^{+/-}$ (**A**) and β4GalT-I$^{-/-}$ (**B**) mice at 25 weeks of age were fractionated by gel filtration and the IgA levels in each fraction were measured. **Arrowheads** indicate 440 kd, and **arrows** indicate 150 kd. **C:** Fractions 16, 20, and 25 of the **A** (+/−) and **B** (−/−) samples were separated by electrophoresis under reducing conditions, and Western blot analysis was performed using anti-mouse IgA α-chain antibody. **D:** Western blot analysis of the same samples in **C** separated by electrophoresis under nonreducing conditions.

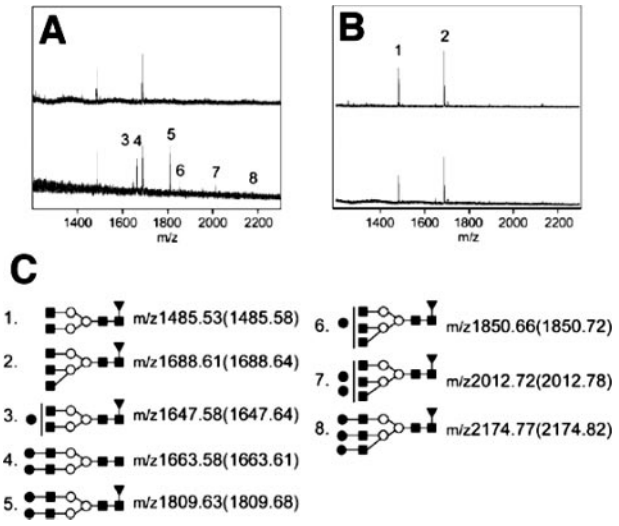

Figure 7. MALDI-TOF mass spectra of *N*-glycans released from IgA. All spectra were acquired with positive mode. Top: Before sialidase digestion; bottom, after sialidase digestion on each panel. **A** and **B:** *N*-glycans on IgA from β4GalT-I$^{+/-}$ and β4GalT-I$^{-/-}$ mice, respectively. Peaks labeled with Arabic numerals were interpreted on **C** according to previous reports.[31] **C:** Proposed structures and their theoretical *m/z* values for the observed signals. Values in parentheses are the observed *m/z* values. All signals were detected as $[M+Na]^{+}$ ions. **Filled squares:** GlcNAc; **open circles:** Mannose; **filled circles:** Galactose; **filled triangles:** Fucose.

glycosylation on human IgA1 has been suggested to be involved in the pathogenesis of human IgAN, because such abnormal IgA1 is detected in the sera of IgAN patients.[20–24] In addition, enzymatically deglycosylated IgA1 forms self-aggregates, adheres to extracellular matrix proteins, and accumulates in rat glomeruli.[46,47] Another group reported that circulating immune complexes in the sera of IgAN patients consist of IgA- and IgG-type antibodies against exposed GalNAc residues in the *O*-glycans on IgA1.[48] Unlike human IgA1, however, mouse IgA does not have *O*-glycosylation sites in its hinge region, but it does have two *N*-glycosylation sites in its CH1 and CH3 regions.[49] Thus, we suppose that carbohydrates, whether they are *O*-glycans or *N*-glycans, of IgA might be involved in the development of IgAN in both humans and mice. Although many studies have focused on the aberrant *O*-glycosylation of IgA in human IgAN, there are several reports suggesting that the *N*-glycosylation on serum IgA from IgAN patients is also defective.[50,51] This study, therefore, suggests that truncation of not only the *O*-glycans but also the *N*-glycans of IgA might participate in the development of IgAN in humans and argues that the *N*-glycans on IgA in the sera from IgAN patients should be analyzed in further detail. An infant patient with a mutation in the β4GalT-I gene, designated as a CDG-IId mutation, was reported to suffer from severe psychomotor retardation and muscle weakness.[52] Because only a single infant patient has been identified to date, further studies are necessary to clarify whether the human mutation in the β4GalT-I gene will cause an IgAN-like disease or not.

Acknowledgments

We thank Drs. S. Nagata (Osaka University) and H. Iwase (Kitazato University) for critical reading of the manuscript; Drs. S. Ogawa and Y. Kitao (Kanazawa University) for their help with fluorescence microscopy; Drs. H. Yamamoto and S. Sakurai (Kanazawa University) for use of the SMART system; Drs. K. Furuichi and K. Kitagawa (Kanazawa University) for their help with quantitative analysis of glomerular sclerosis; and all of the members of the Division of Transgenic Animal Science for their excellent animal care.

References

1. Granovsky M, Fata J, Pawling J, Muller WJ, Khokha R, Dennis JW: Suppression of tumor growth and metastasis in Mgat5-deficient mice. Nat Med 2000, 6:306–312
2. Yoshida A, Kobayashi K, Manya H, Taniguchi K, Kano H, Mizuno M, Inazu T, Mitsuhashi H, Takahashi S, Takeuchi M, Herrmann R, Straub V, Talim B, Voit T, Topaloglu H, Toda T, Endo T: Muscular dystrophy and neuronal migration disorder caused by mutations in a glycosyltransferase, POMGnT1. Dev Cell 2001, 1:717–724
3. Chui D, Oh-Eda M, Liao YF, Panneerselvam K, Lal A, Marek KW, Freeze HH, Moremen KW, Fukuda MN, Marth JD: Alpha-mannosidase-II deficiency results in dyserythropoiesis and unveils an alternate pathway in oligosaccharide biosynthesis. Cell 1997, 90:157–167
4. Wagner R, Matrosovich M, Klenk HD: Functional balance between haemagglutinin and neuraminidase in influenza virus infections. Rev Med Virol 2002, 12:159–166
5. Kawakubo M, Ito Y, Okimura Y, Kobayashi M, Sakura K, Kasama S, Fukuda MN, Fukuda M, Katsuyama T, Nakayama J: Natural antibiotic function of a human gastric mucin against Helicobacter pylori infection. Science 2004, 305:1003–1006
6. Nagamune K, Acosta-Serrano A, Uemura H, Brun R, Kunz-Renggli C, Maeda Y, Ferguson MA, Kinoshita T: Surface sialic acids taken from the host allow trypanosome survival in tsetse fly vectors. J Exp Med 2004, 199:1445–1450
7. Aebi M, Helenius A, Schenk B, Barone R, Fiumara A, Berger EG, Hennet T, Imbach T, Stutz A, Bjursell C, Uller A, Wahlstrom JG, Briones P, Cardo E, Clayton P, Winchester B, Cormier-Dalre V, de Lonlay P, Cuer M, Dupre T, Seta N, de Koning T, Dorland L, de Loos F, Kupers L, Fabritz L, Hasilik M, Marquardt T, Niehues R, Freeze H, Grünewald S, Heykants L, Jaeken J, Matthijs G, Schollen E, Keir xKeir G, Kjaergaard S, Schwartz M, Skovby F, Klein A, Roussel P, Körner C, Lübke T, Thiel C, von Figura K, Koscielak J, Krasnewich D, Lehle L, Peters V, Raab M, Saether O, Schachter H, Van Schaftingen E, Verbert A, Vilaseca A, Wevers R, Yamashita K: Carbohydrate-deficient glycoprotein syndromes become congenital disorders of glycosylation: an updated nomenclature for CDG. First International Workshop on CDGS. Glycoconj J 1999, 16:669–671
8. Hennet T: The galactosyltransferase family. Cell Mol Life Sci 2002, 59:1081–1095
9. Narimatsu H, Sinha S, Brew K, Okayama H, Qasba PK: Cloning and sequencing of cDNA of bovine N-acetylglucosamine (beta 1-4)galactosyltransferase. Proc Natl Acad Sci USA 1986, 83:4720–4724
10. Humphreys-Beher MG, Bunnell B, vanTuinen P, Ledbetter DH, Kidd VJ: Molecular cloning and chromosomal localization of human 4-beta-galactosyltransferase. Proc Natl Acad Sci USA 1986, 83:8918–8922
11. Shaper NL, Hollis GF, Douglas JG, Kirsch IR, Shaper JH: Characterization of the full length cDNA for murine beta-1,4-galactosyltransferase. Novel features at the 5′-end predict two translational start sites at two in-frame AUGs. J Biol Chem 1988, 263:10420–10428
12. Asano M, Furukawa K, Kido M, Matsumoto S, Umesaki Y, Kochibe N, Iwakura Y: Growth retardation and early death of beta-1,4-galactosyltransferase knockout mice with augmented proliferation and abnormal differentiation of epithelial cells. EMBO J 1997, 16:1850–1857
13. Lu Q, Hasty P, Shur BD: Targeted mutation in beta1,4-galactosyltransferase leads to pituitary insufficiency and neonatal lethality. Dev Biol 1997, 181:257–267
14. Asano M, Nakae S, Kotani N, Shirafuji N, Nambu A, Hashimoto N, Kawashima H, Hirose M, Miyasaka M, Takasaki S, Iwakura Y: Impaired selectin-ligand biosynthesis and reduced inflammatory responses in beta-1,4-galactosyltransferase-I-deficient mice. Blood 2003, 102:1678–1685
15. Mori R, Kondo T, Nishie T, Ohshima T, Asano M: Impairment of skin wound healing in beta-1,4-galactosyltransferase-deficient mice with reduced leukocyte recruitment. Am J Pathol 2004, 164:1303–1314
16. D'Amico G: The commonest glomerulonephritis in the world: IgA nephropathy. Q J Med 1987, 64:709–727
17. Galla JH: IgA nephropathy. Kidney Int 1995, 47:377–387
18. Russell MW, Mestecky J, Julian BA, Galla JH: IgA-associated renal diseases: antibodies to environmental antigens in sera and deposition of immunoglobulins and antigens in glomeruli. J Clin Immunol 1986, 6:74–86
19. Floege J, Feehally J: IgA nephropathy: recent developments. J Am Soc Nephrol 2000, 11:2395–2403
20. Mestecky J, Tomana M, Crowley-Nowick PA, Moldoveanu Z, Julian BA, Jackson S: Defective galactosylation and clearance of IgA1 molecules as a possible etiopathogenic factor in IgA nephropathy. Contrib Nephrol 1993, 104:172–182
21. Allen AC, Bailey EM, Barratt J, Buck KS, Feehally J: Analysis of IgA1 O-glycans in IgA nephropathy by fluorophore-assisted carbohydrate electrophoresis. J Am Soc Nephrol 1999, 10:1763–1771
22. Allen AC, Bailey EM, Brenchley PE, Buck KS, Barratt J, Feehally J: Mesangial IgA1 in IgA nephropathy exhibits aberrant O-glycosylation: observations in three patients. Kidney Int 2001, 60:969–973
23. Hiki Y, Odani H, Takahashi M, Yasuda Y, Nishimoto A, Iwase H, Shinzato T, Kobayashi Y, Maeda K: Mass spectrometry proves under-O-glycosylation of glomerular IgA1 in IgA nephropathy. Kidney Int 2001, 59:1077–1085
24. Odani H, Hiki Y, Takahashi M, Nishimoto A, Yasuda Y, Iwase H,

Shinzato T, Maeda K: Direct evidence for decreased sialylation and galactosylation of human serum IgA1 Fc O-glycosylated hinge peptides in IgA nephropathy by mass spectrometry. Biochem Biophys Res Commun 2000, 271:268–274
25. Ando Y, Moriyama T, Miyazaki M, Akagi Y, Kawada N, Isaka Y, Izumi M, Yokoyama K, Yamauchi A, Horio M, Ando A, Ueda N, Sobue K, Imai E, Hori M: Enhanced glomerular expression of caldesmon in IgA nephropathy and its suppression by glucocorticoid-heparin therapy. Nephrol Dial Transplant 1998, 13:1168–1175
26. Wada T, Tomosugi N, Naito T, Yokoyama H, Kobayashi K, Harada A, Mukaida N, Matsushima K: Prevention of proteinuria by the administration of anti-interleukin 8 antibody in experimental acute immune complex-induced glomerulonephritis. J Exp Med 1994, 180:1135–1140
27. Klein-Schneegans AS, Gaveriaux C, Fonteneau P, Loor F: Indirect double sandwich ELISA for the specific and quantitative measurement of mouse IgM, IgA and IgG subclasses. J Immunol Methods 1989, 119:117–125
28. Laemmli UK: Cleavage of structural proteins during the assembly of the head of bacteriophage T4. Nature 1970, 227:680–685
29. Suzuki N, Khoo KH, Chen CM, Chen HC, Lee YC: N-glycan structures of pigeon IgG: a major serum glycoprotein containing Galalpha1-4 Gal termini. J Biol Chem 2003, 278:46293–46306
30. Maeda A, Gohda T, Funabiki K, Horikoshi S, Shirato I, Tomino Y: Significance of serum IgA levels and serum IgA/C3 ratio in diagnostic analysis of patients with IgA nephropathy. J Clin Lab Anal 2003, 17:73–76
31. Lipniunas P, Gronberg G, Krotkiewski H, Angel AS, Nilsson B: Investigation of the structural heterogeneity in the carbohydrate portion of a mouse monoclonal immunoglobulin A antibody. Arch Biochem Biophys 1993, 300:335–345
32. Harvey DJ: Matrix-assisted laser desorption/ionization mass spectrometry of carbohydrates. Mass Spectrom Rev 1999, 18:349–450
33. Wada T, Yokoyama H, Tomosugi N, Hisada Y, Ohta S, Naito T, Kobayashi K, Mukaida N, Matsushima K: Detection of urinary interleukin-8 in glomerular diseases. Kidney Int 1994, 46:455–460
34. Zheng F, Kundu GC, Zhang Z, Ward J, DeMayo F, Mukherjee AB: Uteroglobin is essential in preventing immunoglobulin A nephropathy in mice. Nat Med 1999, 5:1018–1025
35. Launay P, Grossetete B, Arcos-Fajardo M, Gaudin E, Torres SP, Beaudoin L, Patey-Mariaud de Serre N, Lehuen A, Monteiro RC: Fcalpha receptor (CD89) mediates the development of immunoglobulin A (IgA) nephropathy (Berger's disease). Evidence for pathogenic soluble receptor-IgA complexes in patients and CD89 transgenic mice. J Exp Med 2000, 191:1999–2009
36. Wang J, Anders RA, Wu Q, Peng D, Cho JH, Sun Y, Karaliukas R, Kang HS, Turner JR, Fu YX: Dysregulated LIGHT expression on T cells mediates intestinal inflammation and contributes to IgA nephropathy. J Clin Invest 2004, 113:826–835
37. Chui D, Sellakumar G, Green R, Sutton-Smith M, McQuistan T, Marek K, Morris H, Dell A, Marth J: Genetic remodeling of protein glycosylation in vivo induces autoimmune disease. Proc Natl Acad Sci USA 2001, 98:1142–1147
38. Chuang PD, Morrison SL: Elimination of N-linked glycosylation sites from the human IgA1 constant region: effects on structure and function. J Immunol 1997, 158:724–732
39. Royle L, Roos A, Harvey DJ, Wormald MR, van Gijlswijk-Janssen D, Redwan el RM, Wilson IA, Daha MR, Dwek RA, Rudd PM: Secretory IgA N- and O-glycans provide a link between the innate and adaptive immune systems. J Biol Chem 2003, 278:20140–20153
40. Rifai A, Small Jr PA, Teague PO, Ayoub EM: Experimental IgA nephropathy. J Exp Med 1979, 150:1161–1173
41. Miyawaki S, Muso E, Takeuchi E, Matsushima H, Shibata Y, Sasayama S, Yoshida H: Selective breeding for high serum IgA levels from noninbred ddY mice: isolation of a strain with an early onset of glomerular IgA deposition. Nephron 1997, 76:201–207
42. Kobayashi I, Nogaki F, Kusano H, Ono T, Miyawaki S, Yoshida H, Muso E: Interleukin-12 alters the physicochemical characteristics of serum and glomerular IgA and modifies glycosylation in a ddY mouse strain having high IgA levels. Nephrol Dial Transplant 2002, 17:2108–2116
43. Marquina R, Diez MA, Lopez-Hoyos M, Buelta L, Kuroki A, Kikuchi S, Villegas J, Pihlgren M, Siegrist CA, Arias M, Izui S, Merino J, Merino R: Inhibition of B cell death causes the development of an IgA nephropathy in (New Zealand white x C57BL/6)F(1)-bcl-2 transgenic mice. J Immunol 2004, 172:7177–7185
44. Smith AC, Feehally J: New insights into the pathogenesis of IgA nephropathy. Pathogenesis of IgA nephropathy. Springer Semin Immunopathol 2003, 24:477–493
45. Mattu TS, Pleass RJ, Willis AC, Kilian M, Wormald MR, Lellouch AC, Rudd PM, Woof JM, Dwek RA: The glycosylation and structure of human serum IgA1, Fab, and Fc regions and the role of N-glycosylation on Fc alpha receptor interactions. J Biol Chem 1998, 273:2260–2272
46. Kokubo T, Hiki Y, Iwase H, Tanaka A, Toma K, Hotta K, Kobayashi Y: Protective role of IgA1 glycans against IgA1 self-aggregation and adhesion to extracellular matrix proteins. J Am Soc Nephrol 1998, 9:2048–2054
47. Sano T, Hiki Y, Kokubo T, Iwase H, Shigematsu H, Kobayashi Y: Enzymatically deglycosylated human IgA1 molecules accumulate and induce inflammatory cell reaction in rat glomeruli. Nephrol Dial Transplant 2002, 17:50–56
48. Tomana M, Novak J, Julian BA, Matousovic K, Konecny K, Mestecky J: Circulating immune complexes in IgA nephropathy consist of IgA1 with galactose-deficient hinge region and antiglycan antibodies. J Clin Invest 1999, 104:73–81
49. Young NM, Jackson GE, Brisson JR: The glycopeptides of the mouse immunoglobulin A T15. Mol Immunol 1990, 27:1083–1090
50. Baharaki D, Dueymes M, Perrichot R, Basset C, Le Corre R, Cledes J, Youinou P: Aberrant glycosylation of IgA from patients with IgA nephropathy. Glycoconj J 1996, 13:505–511
51. Amore A, Cirina P, Conti G, Brusa P, Peruzzi L, Coppo R: Glycosylation of circulating IgA in patients with IgA nephropathy modulates proliferation and apoptosis of mesangial cells. J Am Soc Nephrol 2001, 12:1862–1871
52. Hansske B, Thiel C, Lubke T, Hasilik M, Honing S, Peters V, Heidemann PH, Hoffmann GF, Berger EG, von Figura K, Korner C: Deficiency of UDP-galactose:N-acetylglucosamine beta-1,4-galactosyltransferase I causes the congenital disorder of glycosylation type IId. J Clin Invest 2002, 109:725–733